ANTIOXIDANTS & REDOX SIGNALING
Volume 12, Number 8, 2010

DOI: 10.1089/ars.2009.2508

ORIGINAL RESEARCH COMMUNICATION

Topoisomerase Inhibitor Coralyne Photosensitizes DNA, Leading to Elicitation of Chk2-Dependent S-phase Checkpoint and p53-Independent Apoptosis in Cancer Cells

Birija Sankar Patro, Biswanath Maity, and Subrata Chattopadhyay

Abstract

The possibility of synergism between the topoisomerase inhibition by coralyne and its DNA photonicking properties being used to kill cancer cells was explored. Compared with coralyne alone, the CUVA treatment dramatically enhanced DNA damage and apoptosis in cells. Despite causing an increased p53 expression, the CUVA treatment led to p53-independent apoptosis, causing almost similar cell death in wild-type, p53 mutant, and p53-silenced tumor cells. Expression of the p53-regulated downstream proteins like p21, and DNA-damage–dependent p53 phosphorylation at serine-15 residue also was not elicited by the CUVA treatment, at a low coralyne concentration. Instead, it led to an immediate activation of the Chk2-mediated S-phase arrest, despite activating PARP protein for DNA repair. The S-phase arrest subsequently ensures apoptosis through activation of caspases-3 and -9, the latter being reflected from the results with a specific caspase-9 inhibitor. Abrogation of Chk2 activity by shRNA or by using ATM-specific inhibitor (ATMi) led to a defective S-phase checkpoint and further augmentation in apoptosis. However, at a high coralyne concentration, the CUVA-induced apoptosis followed multiple and independent pathways, involving several caspases. The CUVA treatment may represent a novel mechanism-based protocol for increasing the efficacy of coralyne in inducing apoptosis in both p53 wild-type and mutant tumor cells. *Antioxid. Redox Signal.* 12, 945–960.

Introduction

Most of the cancer therapeutic armamentarium induces DNA damage that triggers a p53-dependent apoptotic response. However, the p53 tumor-suppressor gene is mutated in up to 50% of human tumors (41), which may contribute to resistance to various types of therapies (1, 4, 16). Identifying drugs that induce p53-independent apoptosis is therefore important. Conversely, many cancer cells with deregulated but exquisite modulations of oncogenes are treading on thin ice, as they ought to preserve genome integrity for continuous and undisrupted cell divisions. The key molecular components, which act in response to DNA damage, are the checkpoint responses (23). The activation of checkpoints due to DNA damage leads to Chk2-p53-p21–dependent G_1 arrest, and p53-independent Chk2-NBS1/BRCA1 mediated S-phase or Chk1/Chk2-cdc25c–mediated G_2 arrest. These checkpoints either arrest cell-cycle progression, allowing DNA repair if the damage is not severe, or produce apoptosis if the damage is terminally irreversible (12, 47). Although many drugs are reported to trigger the DNA damage–induced checkpoint activation or apoptosis or both, most of these have narrow therapeutic windows: a too-low dose leads to repairable DNA damage and hence no effect, whereas a too-high dose leads to mass destruction of even normal cells (12, 25, 48). Achieving a higher degree of DNA damage with a lower concentration of any drug, which might force cells into an apoptotic program, would have immense potential to enhance its efficacy and to limit side effects.

Protoberberine alkaloids and their derivatives are used as antitumor agents in traditional medicine and have been investigated in modern times (11, 35, 52). The antineoplastic activity of these alkaloids and their congeners are derived from their abilities to bind to DNA and inhibit the topoisomerase I enzyme (15, 31). However, minor alterations in their chemical structures significantly affect the relative efficacy of the analogues as topoisomerase poisons (26). Although berberine is the most studied among these alkaloids,

Bio-Organic Division, Bhabha Atomic Research Centre, Mumbai, India.

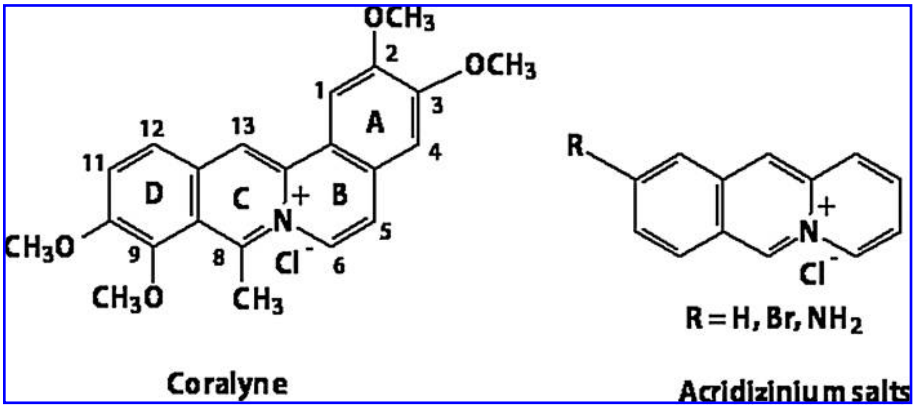

FIG. 1. Chemical structures of coralyne and acridizinium derivatives.

its synthetic congener, coralyne (Fig. 1), has more-pronounced antitumor activity. Studies performed with coralyne and several of its derivatives suggested the importance of the C-8 methyl substituent and C-5, C-6 unsaturation in the protoberberines for their antitumor activity against L1210 and P388 leukemias in mice (50, 51).

Protoberberines also are known to generate various reactive oxygen species (ROS) in the presence of UV (ultraviolet) light (7), whereas coralyne and some related compounds show the DNA photonicking ability (21, 22, 45, 46). Whether the DNA-damaging property of any single drug could successfully be combined with its photochemotherapy has not even begun to be explored. Currently, two different phototherapeutic approaches, (a) photodynamic therapy (PDT) involving porphyrins and related compounds along with infrared radiation; and (b) psoralen derivatives and UVA (320 to 400 nm), the so-called PUVA therapy, are used to treat some types of cancer. Specifically, PUVA treatment is used for psoriasis, cutaneous T-cell lymphoma, and chronic graft-*versus*-host disease (10). Although effective, PUVA has serious limitations, particularly with the p53 mutant cells, requiring a high cumulative dose of UVA. For this reason, alternative ways must be found to kill cancer cells through p53-independent method at a lower dose of the DNA-damaging drugs.

Very recently, a possible alternative approach of using thiothymidine along with UVA in the treatment of certain cancers has been reported (33). Also, the DNA photonicking agents, such as the acridizinium salts, have been suggested to be useful in the photochemotherapy of cancer (5). Because the acridizinium salts are structurally similar to coralyne (Fig. 1), except for the differences in the A-ring and substituents, we envisaged a similar activity of coralyne. Given that the topoisomerase inhibitors accumulate in high concentrations in and around DNA, it might be interesting to couple the bioactivity of these molecules with their photosensitizing property to perturb normal DNA functioning and to achieve synergism in killing cancer cells. This might assist in achieving therapeutic benefits of the drug, even at a lower concentration. With this hypothesis, we explored the possibility of synergism between the known topoisomerase inhibitory and the possible DNA photonicking properties of coralyne to kill cancer cells. For a better understanding of molecular mechanism, its photosensitizing ability was studied in detail in cellular conditions. The combined treatment with coralyne and UVA is referred to as CUVA throughout this study.

Materials and Methods

Materials

Coralyne (purity >99%), 8-methoxypsoralen (8-MOP), LMP agarose, fetal bovine serum (FBS), DMEM, RPMI-1640, penicillin, streptomycin, MTT [3-(4,5-dimethylthiazol-2-yl)-2,5-diphenyltetrazolium bromide], 3-AB (3-aminobenzidine), nocodazole, Z-VAD-FMK, Z-DEVD-FMK, Z-IETD-FMK, and Z-LEHD-FMK, antibodies for p21, p53, and β-actin, as well as kits for caspase-3, caspase-8, and caspase-9 were purchased from Sigma-Aldrich (St. Louis, MO). Other materials used were propidium iodide, G418 sulfate, a kit for determination of phosphorylation of the serine 15 moiety of p53, and the antibodies for phospho-Chk2 (Santa Cruz Biotechnology, Santa Cruz, CA), phospho-317-Chk1, phospho-p53, and PARP (Cell Signaling Technology, Inc., Danvers, MA), phospho-ATM (Millipore, Billerica, MA), and Chk2 (Calbiochem, San Diego, CA). [^{14}C]Thymidine ([^{14}C]TdR, 50 μCi) and ^{3}H-thymidine ([^{3}H]TdR, 50 μCi) were obtained from American Radiolabeled Chemicals, Inc., (St. Louis, MO) and Board of Radiation & Isotope Technology, Mumbai, India, respectively. All the cell lines were procured from the National Centre for Cell Science (NCCS), Pune, India. ATM-specific inhibitor (ATMi, 118500) and Chk2-specific inhibitor (Chk2i, 220485) were purchased from Calbiochem. A 20-m*M* stock solution of coralyne was prepared in warm water and used within 7 days. 8-MOP, ATMi, Chk2i, and camptothecin (CPT) were dissolved in dimethyl sulfoxide at 1 mg/ml.

UVA treatment

The UVA light from four Phillips lamps (each 25 W) was passed through Schott WG 335 filters and a glass shield to provide a UV wavelength >360 nm. The distance between the UV source and the surface of the irradiated solutions was kept at 5 cm to maintain the UV dose rate at 4 J/m^2/s. The UV fluence was quantified with a research radiometer (IL 1700; International Light, Newburyport, MA).

Cell culture and coralyne, psoralen, CUVA, or PUVA treatment conditions

The human breast adenocarcinoma (MDA-MB-231 and MCF-7) and skin epidermoid carcinoma (A431) cell lines were cultured in DMEM medium, whereas the human lung carcinoma (A549) and human normal kidney (HEK293) cell lines

were cultured in RPMI medium supplemented with 10% FBS at 37°C in a 5% CO_2 atmosphere. For coralyne or CUVA treatment, the overnight-grown unsynchronized cells were treated with different concentrations of coralyne for 2 h in PBS. The cells were washed twice with PBS, and either kept in PBS for 0.5 h in case of coralyne treatment, or irradiated with the UVA set up for 0.5 h in PBS for the CUVA treatment. Subsequently, PBS was removed from the treatments, and the cells were incubated in a regular medium at 37°C in a 5% CO_2 atmosphere for the time specified in the respective figure legends and text. For the psoralen or PUVA treatment, cells were treated similarly, except for using psoralen instead of coralyne.

MTT and cell-proliferation assay

The cytotoxic effects of coralyne, psoralen, CUVA, and PUVA treatment were determined by the MTT method, as described earlier (29).

Comet assay

The DNA damage in the coralyne- or CUVA-treated A549 cells was monitored with the alkaline comet assay, as described earlier (34). For each condition, the Olive-tail moments (extent of DNA damage) were measured in a total of 300 randomly chosen cells by using Comet Assay IV software (Perceptive Instruments, Suffolk, U.K.). For the DNA-repair studies, the A549 cells were incubated with PARP-1 inhibitor (3-AB, 4 m*M*) for 1 h before the CUVA treatment.

Measurement of apoptosis with ELISA

The apoptosis induction by coralyne or the CUVA treatment was assessed by using a Cell Death ELISA^{PLUS} kit (Roche Molecular Biochemicals, Indianapolis, IN). The kit uses a photometric enzyme immunoassay that quantitatively determines the enrichment of cytoplasmic histone-associated DNA fragments (mono- and oligosomes) after apoptotic cell death.

Measurement of caspase activities and their inhibition

The assays of the caspase activity were based on spectrophotometric detection of the chromophore pNA after its cleavage from the labeled substrate Ac-LEHD-pNA, Ac-DEVD-pNA, and Ac-IETD-pNA by caspase-9, caspase-3, and caspase-8 proteases, respectively. Assays were performed with the caspase-3 and caspase-8 colorimetric kits (Sigma-Aldrich) or caspase-9 substrate (Sigma-Aldrich) according to the manufacturer's protocol. For the caspase-inhibition studies, cells were treated with inhibitory peptides Z-DEVD-FMK (a cell-permeable inhibitor of caspase 3, 6, 7, 8, and 10), Z-VAD-FMK (caspase-3 inhibitor), Z-IETD-FMK (caspase-8 inhibitor), or Z-LEHD-FMK (caspase-9 inhibitor). The inhibitors were present throughout the experiment, including the 2-h preincubation period before coralyne or CUVA treatment.

Western blot analysis

Preparations of protein samples and Western blots were performed as described previously (19). The bands were quantified with respect to β-actin bands, by using Kodak Gelquant software. The values (arbitrary unit, mean ± SEM) are the density-scanning results of three independent experiments, considering that of untreated control cells as 1.

Assay of DNA synthesis by [^{3}H]thymidine incorporation

A549 cells were prelabeled for 48 h with [^{14}C]TdR (10 nCi/ml) and pulse-labeled for the last 10 min with [^{3}H]TdR (1 μCi/ml) during the respective recovery periods from coralyne and CUVA treatments. Further incorporation was stopped by washing the cells twice with cold PBS. Subsequently, the cells were scraped into 2 ml cold PBS; aliquots were precipitated with 100% trichloroacetic acid in triplicate. Every 10 min, samples were vigorously vortexed for 2 h. After centrifugation at 9,400 *g* for 10 min at 4°C, 0.5 ml of 0.4 *M* NaOH was added to the pellets and kept overnight at 37°C to dissolve the precipitates. Samples were counted by using dual-label liquid scintillation, and the DPM of [^{3}H]TdR was normalized to that of [^{14}C]TdR in each sample. DNA synthesis was measured in terms of $^3H/^{14}C$ in the treated samples divided by $^3H/^{14}C$ in the untreated controls (36).

Transfection of A549 cells

The A549 cells were transfected with plasmids purchased from Imgenex (San Diego, CA) encoding short-hairpin RNA (shRNA) specific for p53 (pSuppressorNeo-p53), Chk2 (pSuppressorNeo-Chk2), or the nonspecific control plasmid (pSuppressorNeo-con). The nonspecific control plasmid is identical to pSuppressorNeo-Chk2 and pSuppressorNeo-p53, except that it contains a scrambled sequence with no significant homology to rat, mouse, and human gene sequences. The A549 cells were transfected with a pSuppressorNeo-con, pSuppressorNeo-Chk2, or pSuppressorNeo-p53 plasmid by using DOTAP liposomal transfection reagent (Roche Molecular Biochemicals, Indianapolis, IN), as described in the manufacturer's protocol. The transfected cells were grown for 3 weeks in a medium containing 800 μg G418/ml. Several G418-resistant clones were expanded and screened for the p53 and Chk2 proteins. The clone with the lowest expression was selected for the studies and was maintained further in the presence of 500-μg G418/ml.

Flow-cytometry analysis

Cells were treated with coralyne or CUVA at a 0.2 μM concentration of coralyne. In a separate set, cells were pretreated with Chk2-specific inhibitor (Chk2i, 100 n*M*) for 2 h, and subsequently, Chk2i was included throughout the experiment. The untreated and treated cells were allowed to recover in complete medium containing nocodazole (0.25 μg/ml) for 24 h. Cells were trypsinized, washed with PBS, and single cells were fixed with chilled 80% ethanol for at least 3 h at −20°C. The staining was performed for 30 min at room temperature in PBS containing 20 μg/ml propidium iodide and 50 μg/ml RNase. Data were collected with a Becton Dickinson FACS machine (Mountain View, CA). Cell-cycle analysis was performed by using FlowJo software, in which doublets and debris were excluded by software algorithms.

Clonogenic survival assay

Reproductive cell death was assayed by measuring colony formation with and without coralyne, psoralen, CUVA, or PUVA treatment, as described earlier (2).

Statistical analyses

For all the tests, the level of statistical significance was set at $p < 0.05$. When needed, the data were transformed to achieve a normal distribution. The one-way ANOVA was used to test the significance of differences in measured variables between the control and the treated groups.

Results

Photosensitizing effect of CUVA treatment on different cancer cells

The photosensitizing ability of the CUVA treatment on two p53 wild-type (A549 and MCF7) and two p53 mutant (A431 and MDA-MB-231) cells was studied with the MTT assay. This assay was carried out by using different UVA exposure times (0 to 14 kJ/m^2) and various concentrations of coralyne. The representative results obtained for 7 kJ/m^2 of UVA are shown in Fig. 2A through D. Irrespective of the cell lines used, various combinations of CUVA showed better cell killing compared with the treatment with coralyne alone. UVA exposure alone (7 kJ/m^2) did not cause any appreciable loss in cell survival of all the four cell lines (data not shown). The CUVA protocol (up to 2 μM) did not show significant toxicity to the HEK293 (human normal kidney) cell lines in the MTT assay.

In the p53 wild-type A549 and MCF7 cancer cells, the SF_{80} values (coralyne concentration at which 80% cells survived) for the CUVA treatment were 0.015 and 0.014 μM, whereas those for coralyne treatment were 15.86 and 21.15 μM, respectively (Fig. 2A and B). With the p53 mutant A431 and MDA-MB-231 cancer cells, the SF_{80} values for CUVA treatment were 0.4 and 0.04 μM, and for coralyne treatment were 12.36 and 24.17 μM (Fig. 2C and D). Notably, these represent about 1,057-, 1,510-, 31-, and 604-fold enhanced sensitivity of A549, MCF7, A431, and MDA-MB-231 cells to the CUVA treatment compared with treatment with coralyne alone. In control experiments, coralyne did not sensitize the cells when added after UVA exposure (data not shown), revealing that the photosensitization effect requires the prior presence of coralyne in the system. Comparison of the photosensitizing efficacies of the CUVA and PUVA treatments revealed the former to be about10- to 15-fold more effective in reducing the viability of A549 and MDA-MB-231 cells (Fig. 3A and B).

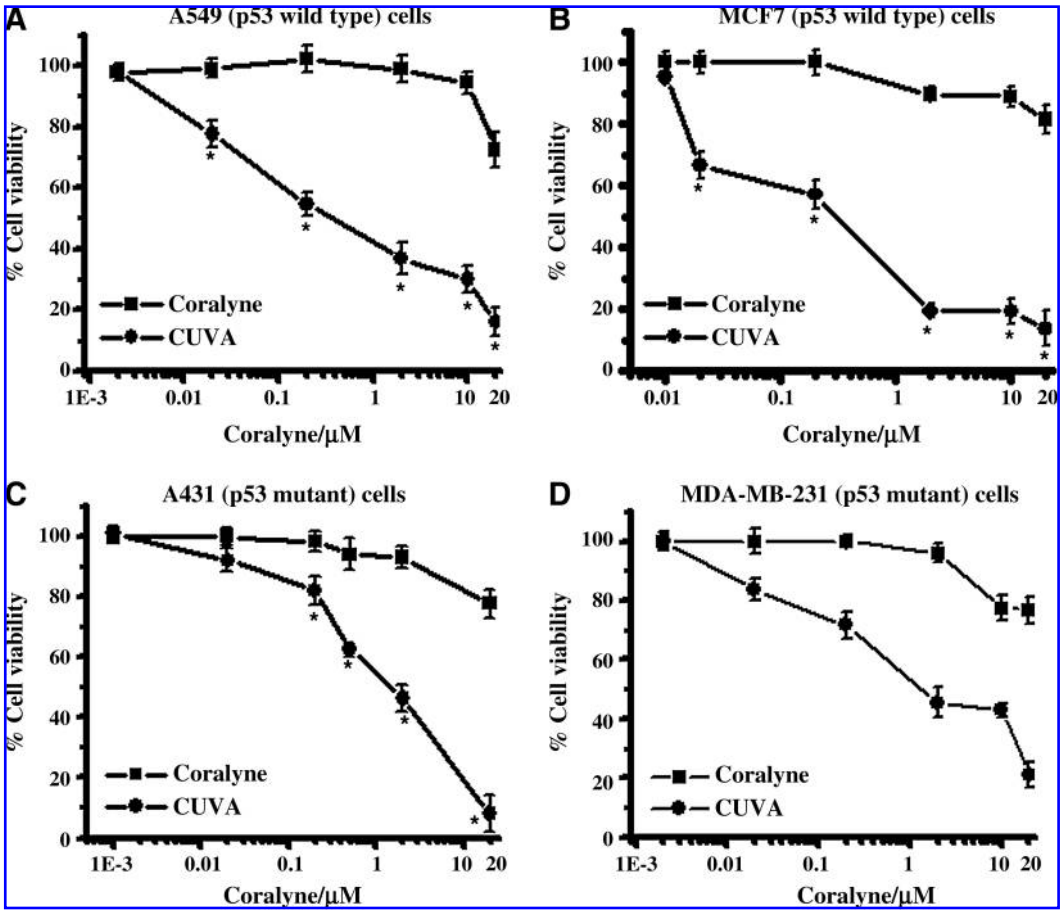

FIG. 2. Growth inhibition of p53 wild-type and *p53* mutant cells by coralyne and CUVA treatment. (**A**) A549 (p53 wild-type); (**B**) MCF7 (p53 wild-type); (**C**) A431 (p53 mutant); and (**D**) MDA-MB-231 (p53 mutant). The cells grown in 96-well plates (10^4 cells/well) were treated with coralyne alone or CUVA and subsequently incubated for 72 h. Cell viability was assessed with the MTT assay, and the results are expressed in percentages, considering that of the untreated control cells as 100. The experiments were repeated 3 times with similar results; all determinations were made in six replicates; and the *error bars* show the standard errors.

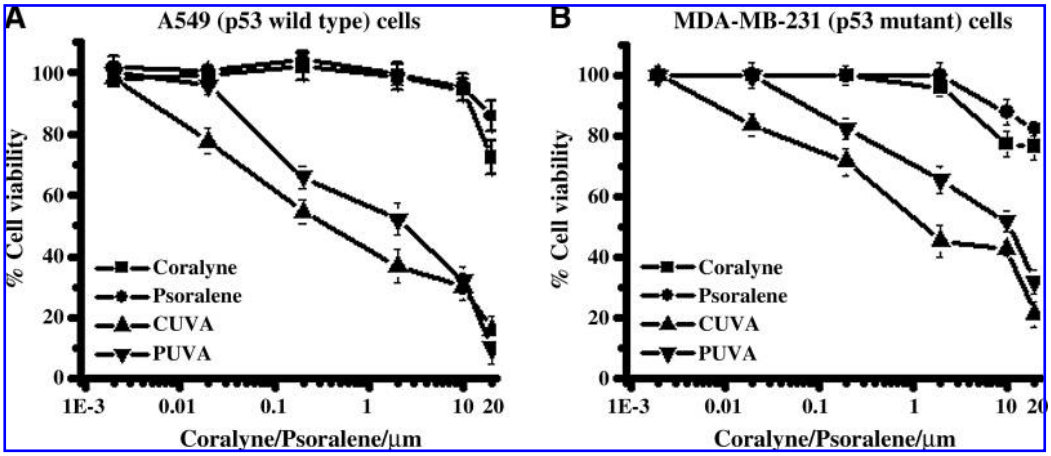

FIG. 3. Growth inhibition in p53 (wild-type) and *p53* (mutant) cells by CUVA and PUVA. (**A**) A549 (p53 wild-type) and (**B**) MDA-MB-231 (*p53* mutant) cells grown in 96-well plates (1×10^4 cells/well) were treated with coralyne, psoralen, CUVA, or PUVA and then incubated for 72 h. Cell viability was assessed with the MTT assay, as described under Experimental Procedures, and the results are expressed in percentages, considering that of the untreated control cells as 100. The experiments were repeated 3 times with similar results, and all determinations were made in triplicate. *Error bars,* standard errors.

Role of p53 in the CUVA-induced cell death

To confirm the actual role of p53 in the CUVA-induced death process, we depleted p53 mRNA in the A549 cells by RNA interference. The respective A549 cells expressing antisense p53 or scrambled negative control product are designated as A549-p53 or A549-con cells throughout this report. The p53 depletion in the A549-p53 cells was confirmed with immunoblot (Fig. 4A). Subsequently, the effects of coralyne and CUVA treatment on long-term survival of A549 and A549-p53 cells was assessed with the clonogenic assay. Compared with that of the untreated A549-con cells, treatment with coralyne (0.02, 0.2, and 20 μM) inhibited the colony formation to 99%, 85%, and 55%, respectively on day 12. The CUVA treatment (7 kJ/m^2 UVA) at the same concentrations of coralyne reduced it to about 62%, 44%, and 1%, respectively, clearly revealing its supremacy over coralyne-alone treatment in inducing the death of the A549 cells (Fig. 4B). With A549-p53 cells, similar results were observed (Fig. 4B and C).

Next, the A549, A549-con, and A549-p53 cells were treated with different concentrations (0, 0.02, 0.2, and 20 μM) of coralyne alone or CUVA, and the induction of p53 expression was measured with ELISA. Treatment of A549 cells with coralyne or CUVA increased the p53 expression by 1.2- to 1.6-fold, at 3 h after treatment, and the effect was dependent on coralyne concentrations. At 12 h after treatment with coralyne, the p53 expression was increased further to 1.5- to 1.9-fold, whereas the same for the CUVA treatment was 2.0- to 2.6-fold (Fig. 5A). Our Western blot results (Fig. 5C) were in good correlation with the ELISA data. A similar trend of p53 expression also was observed with A549-con cells (data not shown). However, the dose- and time-dependent increase in p53 expression was almost abolished in the A549-p53 cells (Fig. 5B).

Subsequently, the differential sensitivity of the A549, A549-con, and A549-p53 cells to the CUVA treatment was checked by comparing their survival losses. CUVA treatment reduced the cell survival of the A549-con, A549-p53, and the untransfected A549 cells to the same extent. The SF_{80} doses for A549, A549-con, and A549-p53 cells in coralyne-alone treatment were about 16.56, 14.88, and 14.17 μM, whereas those for the CUVA treatment were about 0.016, 0.014, and 0.013 μM, respectively (Fig. 5D). These revealed that the A549, A549-con, and A549-p53 cells were 1,035-, 1,063-, and 1,090-fold more sensitive to the CUVA treatment than to that with coralyne alone.

CUVA treatment induces apoptosis through activation of caspases

To assess whether the cell death induced by the CUVA treatment involves apoptosis, we looked for (a) enrichment of nucleosomes in the cytoplasm, (b) poly(ADP-ribose) polymerase (PARP) cleavage, (c) activation of caspases, and (d) effects of the caspase inhibitors on apoptosis. Treatment of the A549 cells with coralyne (0.002, 0.02, 0.2, and 20 μM) alone increased the accumulation of nucleosomes in the cytoplasm by factors of about 1.0, 0.9, 1.0, and 2.6, respectively, revealing apoptotic killing of the A549 cells by coralyne. In comparison, the CUVA treatment at the same concentrations of coralyne showed enrichment factors of about 0.9, 3.4, 3.9, and 9.2, respectively (Fig. 6A). Thus, the CUVA treatment with even a 1,000-fold less coralyne concentration (0.02 μM) induced more apoptosis than treatment with coralyne (20 μM) alone. Similar results were obtained with the MCF7 and MDA-MB-231 cells (data not shown).

In many systems, the final execution of apoptosis is mediated through caspase-8 and caspase-9 as the initiators, and caspase-3 as the effector. Because PARP is a substrate of caspase-3, we also analyzed the protein level with Western blot. The level of cleaved PARP was also markedly increased by the CUVA treatment, but much less by coralyne alone (Fig. 6B). Next, we assessed the activities and expressions of the caspases-3, -8, and -9 in the coralyne- and CUVA-treated A549 cells. Coralyne (0.2 and 20 μM) alone did not cause any appreciable change in the caspase-3 activity, whereas the CUVA treatment at the same concentrations of coralyne increased it by 1.2- and 2.1-fold, respectively, at 6 h, and by

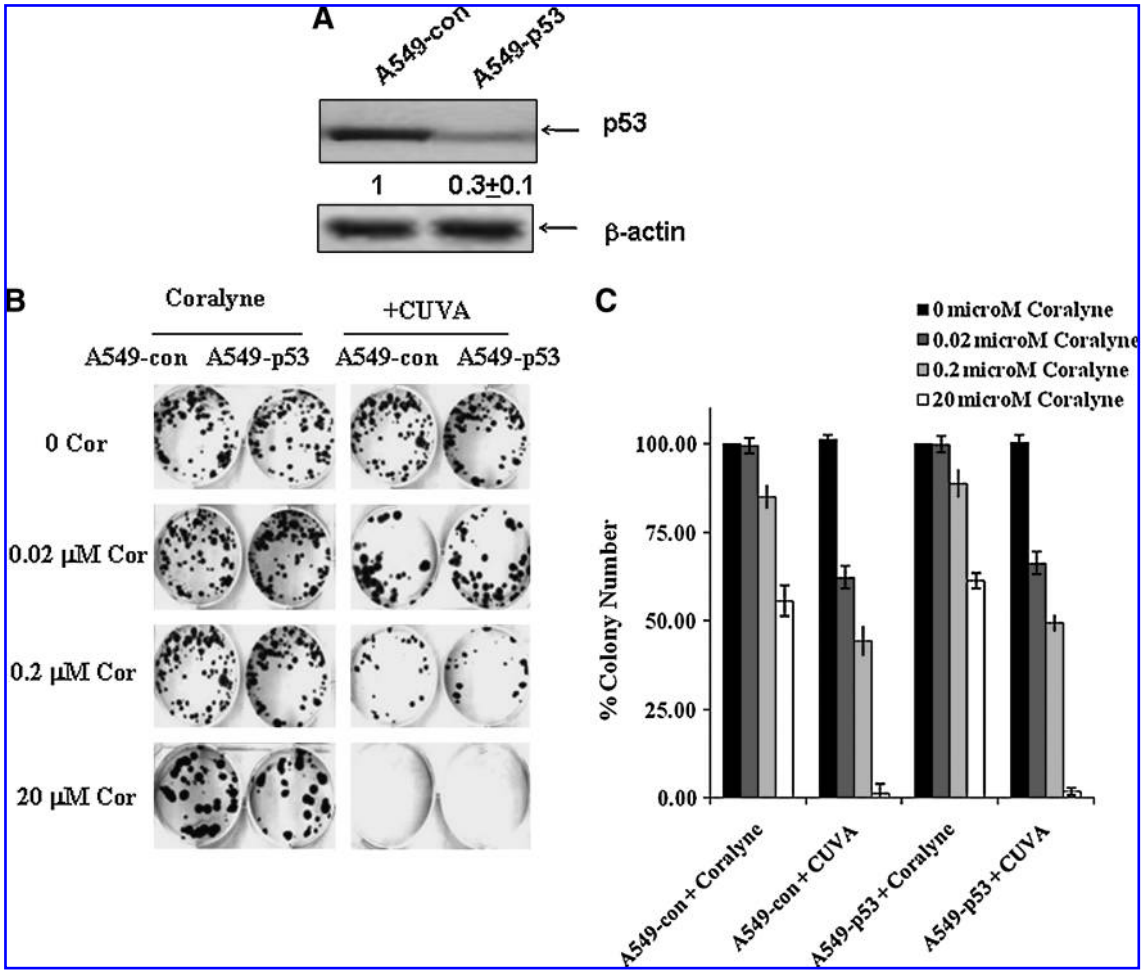

FIG. 4. The p53 depletion does not affect the CUVA-induced cell-death process. (**A**) Western blots of p53: A549-con and A549-p53 cell extracts were probed for the p53 protein levels. (**B**) A549-con and A549-p53 cells grown in Petri plates (300 cells/plate) were treated with coralyne alone or CUVA and incubated for 12 days. Colony formation was assessed as described under Experimental Procedures. (**C**) The quantification data of (**B**). Results are expressed in percentages, considering that of the untreated control cells as 100. These experiments were repeated 3 times with similar results, and all determinations were made in triplicate. *Error bars*, standard errors.

7.7- and 1.9-fold at 24 h (Fig. 7A). Both coralyne alone and CUVA, at a coralyne concentration of 0.2 μM, did not induce caspase-9 activation until 24 h. However, at a concentration of 20 μM, coralyne alone increased the caspase-9 activity marginally (1.5-fold) at 24 h, whereas the CUVA treatment increased the same by 4- and 1.5-fold at 6 h and 24 h, respectively (Fig. 7C). Likewise, when the A549 cells were treated with 0.2 or 20 μM coralyne, the caspase-8 activity did not change significantly. Even the CUVA treatment with 0.2 μM coralyne was ineffective, but it increased the caspase-8 activity by 4.5-fold (6 h) and 6.0-fold (24 h), respectively, at a coralyne concentration of 20 μM (Fig. 7E). The expressions of the individual caspases (Fig. 7B, D, and F) were consistent with their activation by the respective treatments.

For further confirmation of apoptosis in the CUVA-mediated death of A549 cells, the effect of specific caspase inhibitors or a general caspase inhibitor on the frequency of apoptosis (Fig. 8) was monitored 24 h after treating the cells with coralyne or CUVA. For this, the highest nontoxic concentrations of the specific caspases inhibitors (80 μM) and general caspase inhibitor (40 μM) were used. Previously, similar concentrations of caspase inhibitors were used for A549 cells by several groups for this type of study (20, 37). The specific caspase-3 and caspase-9 inhibitors almost completely inhibited the CUVA-induced apoptosis at the lower concentrations (0.02 and 0.2 μM) of coralyne. However, the CUVA-induced apoptosis observed with 20 μM coralyne was partially (about 21%) abrogated by the caspase-9 inhibitor, but not by the caspase-3 inhibitor. This correlates with the observation that CUVA treatment (20 μM coralyne) activated caspase-9, but not caspase-3. In contrast, the caspase-8 inhibitor resulted in only a partial (about 11 to 20%) inhibition of the CUVA-induced apoptosis at all the test concentrations (0.02, 0.2, and 20 μM) of coralyne. Interestingly, the general caspase inhibitor (Z-DEVD-FMK) was more effective than the specific inhibitors in protecting A549 cells against the CUVA-induced apoptosis, irrespective of the coralyne concentrations. As mentioned earlier, coralyne alone could induce appreciable apoptosis in the A549 cells only at a concentration of 20 μM. This was partially inhibited by the caspase-3 and general caspase inhibitors, but not by the caspase-8 and caspase-9 inhibitors. Collectively, the results suggest that

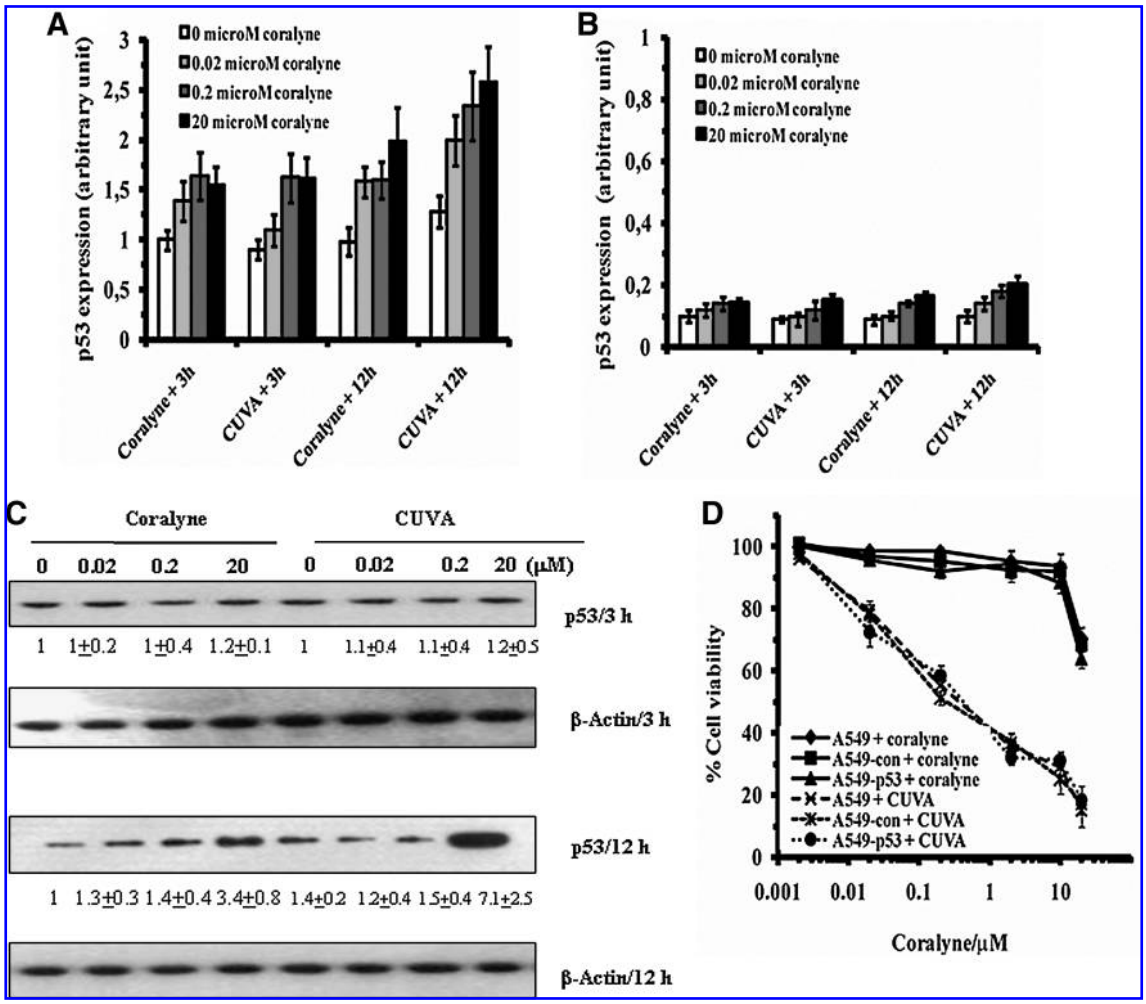

FIG. 5. The p53 expression after the CUVA treatment is dispensable for the CUVA-induced cell-death process. (**A**) ELISA analysis of the p53 expressions in A549 cells. (**B**) ELISA analysis of p53 expressions in A549-p53 cells. Subsequent to the treatment with coralyne or CUVA (at the same coralyne concentration), cellular extracts were prepared and analyzed at 3 h and 12 h. The ELISA results are expressed in an arbitrary unit, considering p53 expression in the untreated control A549 cells as 1. (**C**) Western blot analysis of the p53 expressions in A549 cells after coralyne and CUVA treatment at 3 h and 12 h. (**D**) Analysis of cell viability in A549, A549-con cells, and A549-p53 cells in response to the coralyne alone or to the CUVA treatment. Respective cells grown in 96-well plates (10^4 cells/well) were treated with coralyne alone or CUVA, and subsequently incubated for 72 h. Cell viability was assayed with the MTT method, and the results are expressed in percentages, considering that of the untreated control cells as 100. The experiments were repeated 3 times with similar results; all determinations were made in four replicates. *Error bars,* standard errors.

caspase-3 and caspase-9 play critical roles at lower coralyne concentration (0.02 and 0.2 μM) of the CUVA treatment. At a higher concentration of coralyne (20 μM), several caspases including caspases-3, -8, and -9 are activated through multiple and mostly independent pathways in the CUVA-induced apoptosis in the A549 cells.

DNA damage is the initial key event of apoptosis induction

The involvement of DNA SSB formation in the CUVA-induced apoptosis was studied with the comet assay. Treatment of the A549 cells with coralyne or UVA alone did not result in significant numbers of comet tails, which were observed immediately at 0 h in the CUVA-treated cells. The Olive comet tails moments increased progressively with the increase in the coralyne concentrations (0.02, 0.2, and 20 μM) in the CUVA treatment (Fig. 9A).

The DNA-repair response plays a pivotal role in recovering cells from the DNA damage–induced apoptosis. The conserved nuclear protein, PARP-1, a principal member of a family of DNA-repair enzymes, binds rapidly and directly to both single- and double-strand breaks. PARP-1 inhibition by compounds like 3-aminobenzidine (3-AB) and 4-amino-1,8-naphthalimide (ANI) have been reported to increase the sensitivity of various DNA damage–inducing factors (28, 44). Hence, the possible role of PARP-1 was investigated by studying the effect of 3-AB on CUVA treatment. 3-AB (4 mM), by itself, did not lead to any DNA damage or apoptosis in the A549 cells. However, compared with the untreated cells, a significant amount of DNA damage was still retained in the 3-AB (4 mM)-treated cells after 2 h of the CUVA treatment (Fig.

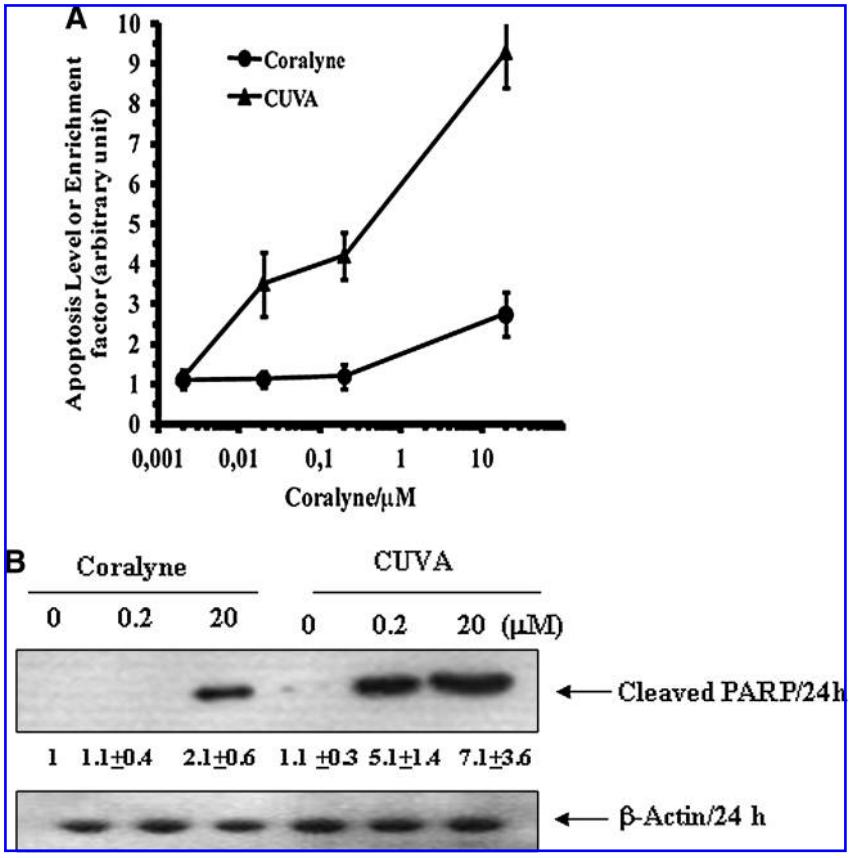

FIG. 6. The CUVA-induced cell death proceeds through apoptosis. (**A**) Analysis of enrichment of nucleosomes in cytoplasm. The A549 cells were treated with coralyne alone or CUVA, and the apoptosis level after 24 h was measured with ELISA. The apoptosis results are expressed in arbitrary units, considering the value of the untreated control cells as 1. (**B**) Western blot analysis of PARP cleavage in A549 cells after coralyne and CUVA treatment at 24 h by Western blotting. All the experiments were repeated 3 times with similar results. All determinations in (**A**) were made in triplicate, and the *error bars* show the standard errors.

9B). In correlation with the DNA-damage results, the CUVA treatment also led to more viability loss in the 3-AB–treated A549 cells than those untreated (Fig. 9C).

CUVA treatment elicits S-phase checkpoint response, and its abrogation by chemical inhibitor or shRNA leads to CUVA-resistance DNA synthesis

Next we investigated whether the CUVA-induced DNA damage results in elicitation of S-phase checkpoints for DNA repair. For this, we measured [^{3}H]thymidine incorporation during DNA synthesis soon after the CUVA treatment in the A549 cells. Treatment with coralyne (0.02 and 0.2 μM) induces a marginal increase in S-phase arrest in the A549 cells up to 2 h. However, when the cells were treated with coralyne (20 μM), the DNA synthesis ([^{3}H]thymidine incorporation) was reduced to about 71% and 66% after 1 h and 2 h, respectively, compared with the untreated cells. In comparison, reduction of the DNA synthesis in the CUVA-treated A549 cells was significantly more even at the lower concentrations of coralyne. At 0.02, 0.2, and 20 μM coralyne, the CUVA treatment reduced DNA synthesis to about 80, 61, and 35% at 1 h, compared with the untreated cells. The corresponding values at 2 h were about 75, 51, and 33%, respectively (Fig. 10A).

For confirming the intra–S-phase arrest as a direct effect of the CUVA rather an indirect and eventual S-phase arrest through sequential activation of p53-p53ser15-p21–mediated G_1 arrest, we monitored DNA synthesis in A549-p53 (*p53* silenced) and MDA-MB-231 (*p53* mutated) cells, immediately (1 h) after the CUVA treatment. These showed results similar to that of the A549 cells (data not shown). No detectable increase in p53 phosphorylation at serine-15 and its downstream target, p21, were observed in the CUVA-treated A549 cells (Fig. 10B and C). Thus, the CUVA treatment arrested the DNA synthesis even in the cells devoid of p53 protein, suggesting its direct role in S-phase arrest without affecting the G_1-phase progress.

Subsequently, the role of CUVA in inducing direct intra–S-phase arrest was probed. Because ATM and ATR kinases play critical roles in inducing intra–S-phase arrest in response to various DNA-damaging agents, we were further interested in knowing the role of ATM or ATR or both in CUVA-induced S-phase arrest. For this, ATM autophosphorylation and Chk2 phosphorylation were checked as a measure of ATM activation. ATR activation was monitored by measuring ATR-specific phosphorylation of Chk1. In response to coralyne (0.2 μM) treatment, the ATM autophosphorylation level increased to 1.3, 1.7, and 1.9 fold after 2 h, 4 h, and 6 h recovery (Fig. 11A). In contrast, CUVA treatment at the same concentration of coralyne caused 3.4-, 2.9-, and 2.7-fold increase in ATM autophosphorylation (Fig. 11A). Similar to these results, Chk2 phosphorylation was also greater in CUVA treatment *vis-à-vis* coralyne-alone treatment (Fig. 11A). Interestingly, although ATR-specific phosphorylation of Chk1 remained unaltered in response to coralyne or CUVA treatment (coralyne, 0.2 μM), the positive control CPT induced ATR-mediated Chk1 phosphorylation (Fig. 11B). These results suggest that the ATM-Chk2 pathway might be critical for the CUVA-induced S-phase arrest.

To ascertain the role of ATM-Chk2 in the CUVA-induced S-phase arrest, A549 cells were treated with ATM-specific inhibitor (ATMi) to reduce the ATM function, or the Chk2

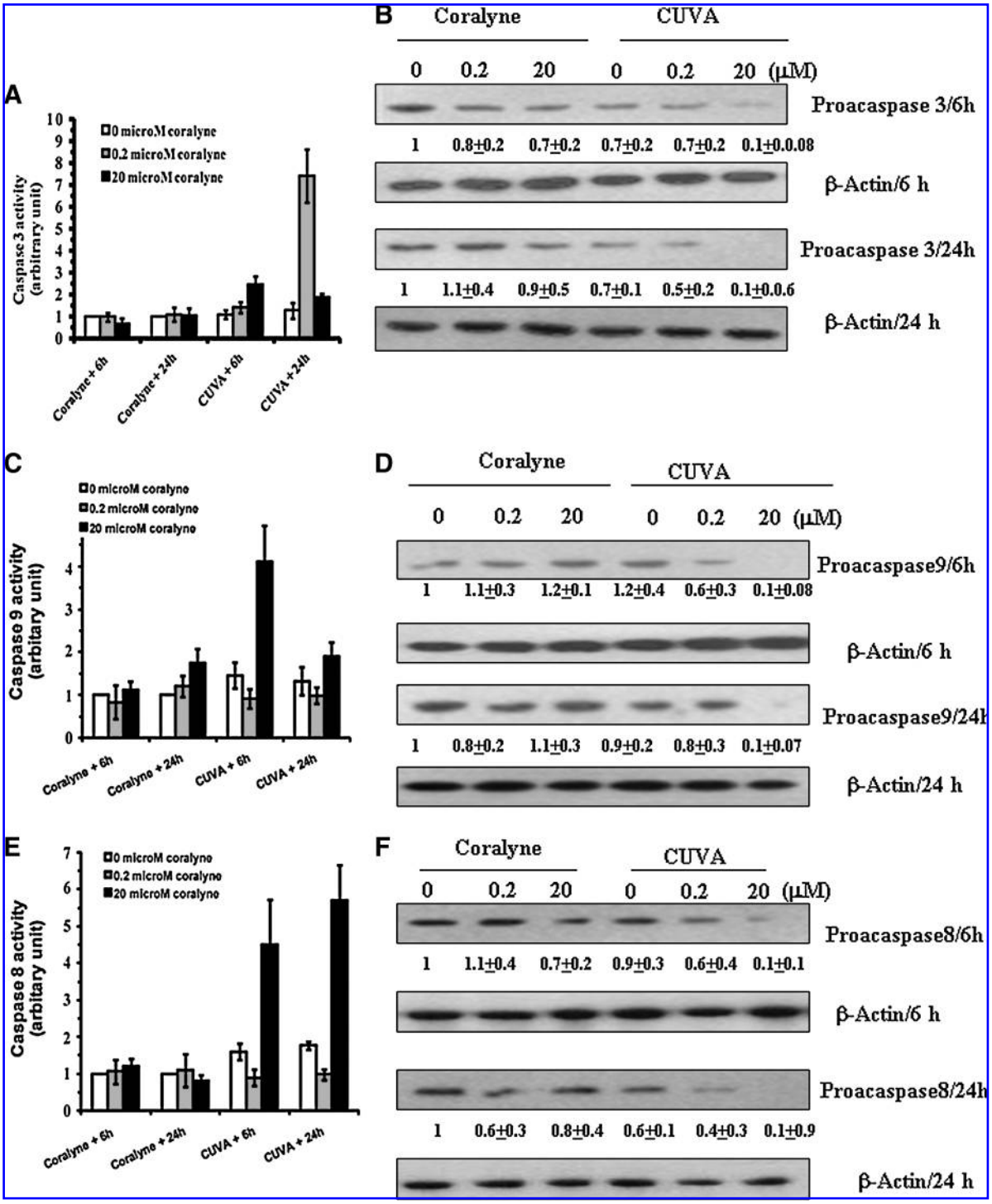

FIG. 7. The CUVA treatment induces apoptosis through differential activation of caspases 3, 8, and 9. ELISA and Western blot analyses of caspase-3 (**A, B**), caspase-9 (**C, D**), and caspase-8 (**E, F**). For the caspases analyses, cellular extracts were prepared at 6 h and 24 h after coralyne and CUVA treatment. The specific caspase activities were analyzed by using ELISA kits. The Western blotting analysis was done for the procaspase cleavage. All the experiments were repeated 4 times with similar results. All determinations in (**A, C**, and **E**) were made in triplicate, and the *error bars* in the ELISA results show the standard errors.

expression was knocked down, and the DNA synthesis in these cells was assessed. For Chk2 silencing, the A549 cells were stably transfected with either the negative control vector or Chk2 shRNA-expressing vector (Fig. 11C). The A549 cells that express antisense Chk2 or scrambled negative control product are designated A549-Chk2 or A549-con cells throughout this report. Western blot experiments showed about 82% depletion of Chk2 protein in the clones of A549-Chk2 cells (selected by G418) compared with that in the parental as well as A549-con cells (Fig. 11C). At the lower

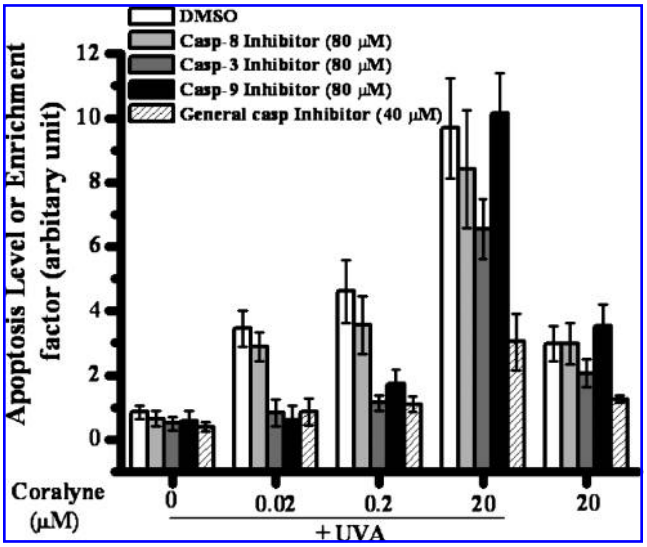

FIG. 8. Different caspase inhibitors alter differently the CUVA-induced apoptosis in A549 cells. The A549 cells pretreated with specific/general caspase inhibitors for 2 h were incubated with coralyne alone or CUVA, and the apoptosis level after 24 h was measured by analyzing the enrichment of nucleosomes in cytoplasm with ELISA. These experiments were repeated 3 times with similar results. The determinations were made in triplicate, and the *error bars* show the standard errors.

concentrations (0.02 and 0.2 μM) of coralyne, the CUVA treatment led to considerable S-phase arrest in the A549-con cells (Fig. 11D), as was observed with A549 cells (Fig. 10A). In contrast, a significant reduction in S-phase arrest was observed in the ATMi-treated and A549-Chk2 cells, under similar conditions (Fig. 11D). Instead, CUVA-resistant DNA synthesis (CUVADS) was observed in these cells (Fig. 11D). This indicated that Chk2 or ATM downregulation enabled the A549 cells to progress through the S phase and to synthesize DNA in response to the CUVA treatment. However, the intra–S-phase arrest, induced by the CUVA treatment at higher concentration of coralyne (20 μM) was not recovered in the ATMi-treated A549-con or A549-Chk2 cells (Fig. 11D). Overall, the CUVA-induced S-phase arrest is ATM and Chk2 dependent at the lower concentrations of coralyne (0.02 and 0.2 μM), and independent at its higher concentration (20 μM).

Further to confirm the CUVA-induced S-phase arrest, we analyzed the cell-cycle profile of A549 cells with flow cytometry. For this, cells were also treated with nocodazole to collect all the cells in the G_2/M phase. This treatment is specifically helpful to monitor S-phase progress in one cell-cycle time (49). In the absence or presence of coralyne (0.2 μM), nocodazole treatment (24 h) did not alter the progress of A549 cells through the S phase (Fig. 11E). However, a significant number of cells were arrested in S phase with CUVA treatment ($40.0 + 7.64\%$) compared with that ($20.32 + 5.64\%$) with coralyne-alone treatment, both with 0.2 μM coralyne (Fig. 11E). Further, Chk2 inhibition by Chk2i led the cells to escape from the CUVA-induced S-phase checkpoint (Fig. 11E). These observations conclusively proved that Chk2 plays an important role in CUVA-induced S-phase arrest.

Depletion of Chk2 Protein Results in Enhanced Apoptosis in A549 Cells

Since loss of checkpoints in cells harboring DNA damage can lead to increased cell death (49), the A549-con, A549-p53 and A549-Chk2 cells were subjected to treatment with coralyne alone or CUVA, and the apoptosis was measured after 24 h. The results showed no significant difference in the coralyne-induced apoptosis in the designated cells. Interestingly, when the cells were treated with CUVA, at 0, 0.002, 0.02, 0.2, and 20 μM coralyne, silencing of Chk2 led to a significant increase in the apoptosis in the A549-Chk2 cells *vis-à-vis* the A549-con and A549-p53 cells (Fig. 12). Taken together, all these results confirmed that the Chk2 protein plays a major role in the CUVA-mediated killing of the A549 cells.

Discussion

The p53 protein is known to be responsible for apoptosis triggered by oncogenes, ionizing radiation, and certain anticancer drugs (39). Patients who have tumors with p53 mutations often have a worse prognosis than do those who have tumors with wild-type p53 (27), resulting in drug resistance (1, 4, 16, 23). Thus, sensitizing cancer cells through the p53-independent pathway is of fundamental importance. Here, we studied the efficacy of CUVA in killing cancer cells both through p53-dependent and -independent pathways, and rationalized its photosensitizing and cytotoxic properties in terms of underlying molecular signaling mechanisms.

With regard to the anticancer property of CUVA, our results with two p53 wild-type and two p53 mutant carcinoma cells established its significantly enhanced cell-killing ability compared with coralyne or UVA treatment alone (Fig. 2). Our initial results, with the p53 mutant (MDA-MB-231 cells) apparently indicated better sensitivity of CUVA toward the p53 wild-type cells. However, the efficacy of the CUVA treatment for the p53 wild-type cells (A549 and MCF7) was only marginally (1.5- to 2.5-fold) better than that for the MDA-MB-231 cells. The poor result with the A431 cells may be due to a low cellular uptake of coralyne. This was also substantiated by the fact that the CUVA treatment caused almost equal and extensive viability loss (Fig. 5D) in both A549 and A549-p53 cells (with 70% less p53 expression than A549 cells), and also reduced the reproductive potential of the A549-con and A549-p53 (*p53* silenced) almost equally (Fig. 4B and C). The superiority of CUVA over PUVA was also evident from our results with A549 (*p53* wild-type) and MDA-MB-231 (*p53* mutated) cells (Fig. 3A and B). However, given that CUVA increased the p53 expression in all the different A549 cells, its partial role in the modulation of the CUVA-induced cell death could not be excluded.

Many studies have demonstrated that apoptosis induction plays the most vital role in cancer treatment with chemotherapy and radiation therapy (13). Hence, we established the involvement of an apoptotic pathway in the CUVA-mediated killing of the A549 cells by the histone-release assay. It is well known that activation of caspases is instrumental in programmed cell death (3). The caspase cascade is initiated by the proteolysis of inactive procaspases and propagated by the cleavage of downstream caspases and substrates, such as PARP (17). Caspase-9 is a member of the CED-3 family and bears high similarity to caspase-3, one of the key executors of apoptosis. Cleavage of procaspase-3 by caspase-9 produces

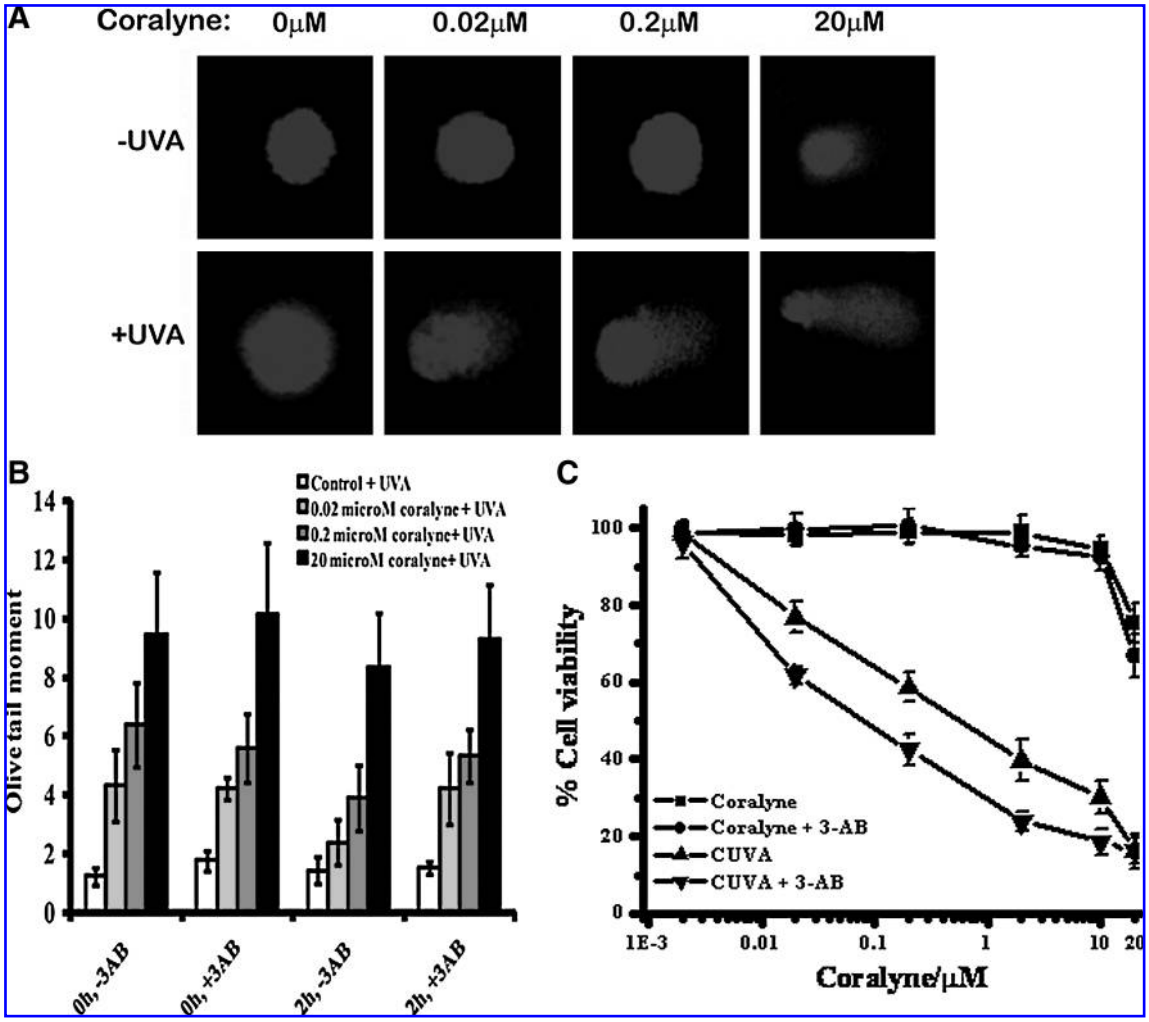

FIG. 9. CUVA treatment causes DNA damage leading to cell death. (**A**) Comet assay analysis of DNA damage. The A549 cells were treated with coralyne alone or with CUVA, and the DNA damage was assessed immediately after the CUVA treatment (0 h). (**B**) Effect of PARP inhibitor (3-AB) on DNA damage. The A549 cells were treated with the CUVA in the absence or presence of 3-AB (4 m*M*). The DNA damage, in terms of average Olive-tail moment, was assessed at 0 h and 2 h by comet assay. The experiments were repeated 4 times with similar results. All determinations were made in triplicate, and the *error bars* show the standard deviations. (**C**) Effect of 3-AB on the CUVA-induced cell-viability loss in A549 cells. A549 cells, preincubated with 3-AB (4 m*M*) for 1 h, were treated with coralyne alone or with CUVA, and then grown for 72 h in the presence of 3-AB. Subsequently, the cell viability was measured with the MTT method. The results are expressed in percentages, considering that of the untreated control cells as 100. All these experiments were repeated 3 times with similar results. The determinations were made in triplicate, and the *error bars* show the standard errors.

an active enzyme that is capable of cleaving PARP. PARP is a chromatin-bound enzyme that, on activation by DNA-strand breaks, catalyzes the successive transfer of ADP-ribose units from NAD to nuclear proteins. Cleavage of PARP results in its inactivation, thereby slowing the DNA-repair process and enhancing apoptosis.

Our results showed that the CUVA-induced apoptosis, at the lower concentrations of coralyne (up to 0.2 μM), was controlled through activation of caspase-3 and caspase-9, with minimal effect from caspase-8. This excluded the operation of a Fas-mediated pathway. Our immunoblots, showing reduced levels of pro-caspase-3 and pro-caspase-9 due to CUVA treatment, were concurrent with the increased activities of the respective caspases (the protein activation is represented by the loss of its pro-form). The cleavage of PARP protein by CUVA also confirmed caspase-3 activation, as PARP is a substrate of caspase-3. Apparently, CUVA first enhances caspase-9 activity in the early apoptotic cascade, which then stimulates the proteolytic activity of other downstream caspases, including caspase-3 (Fig. 7). This, in turn, leads to the cleavage of numerous proteins, including PARP-1. The cleaved product of PARP-1 would enhance the apoptosis process. Although CUVA treatment led to a reduced level of pro-caspase-8 and activation of caspase-8, this may not play a central role in the cytotoxicity of CUVA. Our apoptosis data in the presence of different caspase inhibitors (Fig. 8) also support this. The cytotoxicity of CUVA with coralyne (20 μM) was too high and may involve multiple pathways also involving other caspases. This was evident from the activation of caspase-8 and also the redundancy of the specific caspase inhibitors under this condition.

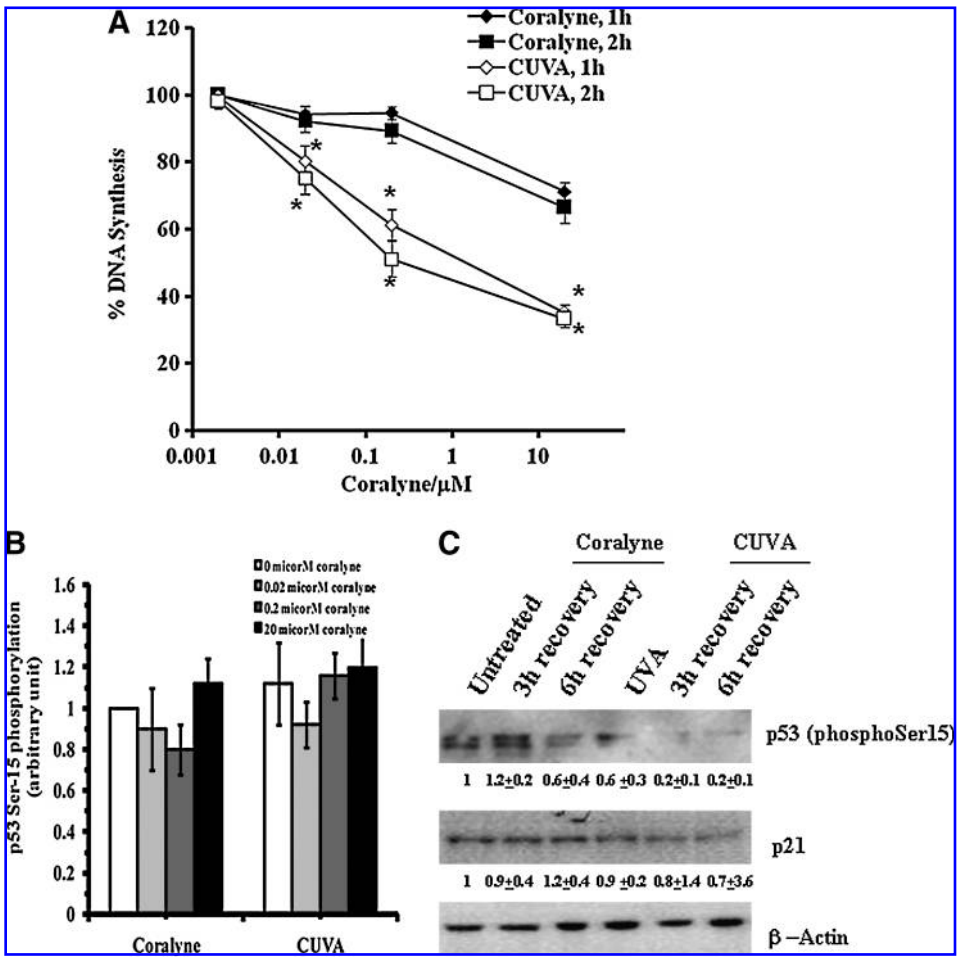

FIG. 10. CUVA treatment elicits an S-phase checkpoint response. (**A**) Analysis of DNA synthesis. The A549 cells were treated with coralyne alone or CUVA, and the DNA synthesis (S phase) was measured after 1 h and 2 h with the [^{3}H]thymidine-incorporation assay, as described under Experimental Procedures. The results are expressed in percentages, considering that of the untreated control cells as 100. *Significantly different compared with the corresponding coralyne-alone samples by one-way ANOVA ($p < 0.05$). (**B**) Analysis of serine-15 phosphorylation in p53. Subsequent to coralyne alone or the CUVA treatment, cellular extracts were prepared at 3 h, and phospho-p53 was analyzed with ELISA. The results are expressed in an arbitrary unit, considering that in the untreated control A549 cells as 1. (**C**) Western blot analyses of expressions of p21 and phosphorylation of serine-15 in p53 after coralyne and CUVA treatment. Subsequent to coralyne-alone or CUVA treatment (0.2 μM coralyne), cellular extracts were prepared at 3 h and 6h, and the expression of p21 proteins or the phosphorylation of serine-15 in p53 was analyzed. These experiments were repeated thrice with similar results. All determinations in (**A**) and (**B**) were made in triplicate, and the *error bars* show the standard deviations.

To address the question of the p53-independent mechanism in the CUVA-induced apoptotic pathway, we envisaged a putative role of *in vivo* DNA photodamage by CUVA. This initial photo event may accumulate DNA lesions, eliciting growth arrest and DNA-repair processes. Failure in the later events would lead to apoptosis. In this respect, our results showed that the CUVA treatment, at all the concentrations of coralyne, led to an instant induction of DNA damage in the A549 cancer cells (Fig. 9A). Besides, pretreatment of the A549 cells with 3-AB (a PARP-1 inhibitor) enhanced the CUVA-mediated cell death (Fig. 9B and C) compared with the untreated cells, possibly because of accumulation of DNA SSBs. These demonstrated that the CUVA treatment could induce cellular DNA lesions in cancer cells, which were not efficiently repaired. This switched the signaling to apoptosis. Cells that are damaged when they are already in the middle of DNA synthesis or replication (S phase) can still elicit intra–S-phase checkpoint signaling events for probable benefit from halting or slowing DNA replication until the damage has been repaired (23). Although the G_1 checkpoint also reduces DNA synthesis, the S-phase checkpoint is a distinct process (23, 40). DNA-synthesis blocks immediately after γ-irradiation is characterized as S-phase arrest, as it reflects the arrest of those cells that are already in S phase rather than an indirect S-phase arrest from the p53-p21–mediated G_1 blocks (8, 24). The possibility of elicitation of intra S-phase checkpoints by CUVA was assessed with [^{3}H]thymidine incorporation into DNA in the A549 cells soon after the CUVA treatment. Coralyne alone could reduce the DNA synthesis only at 20 μM. However, in combination with UVA, its efficacy was seen even at 1,000 times less concentration (Fig. 10A).

One of the first abnormalities to be characterized in cells from cancer-prone individuals affected with ataxia telangiectasia (AT) or Nijmegen breakage syndrome (NBS) is a failure to arrest DNA synthesis even after exposure to ionizing radiation (23, 40). This phenomenon is called "radioresistant DNA synthesis" (RDS). Several lines of evidence implicate the association of AT mutated (ATM) (30), Chk2 (14), NBS1 (25), MRE11 (42), and ATR-Chk1 (36) proteins in the intra–S-phase checkpoint pathway. Our results showed clear evidence that ATR-Chk1 has no role in the CUVA-induced S-phase arrest (Fig. 11A). In the absence of ATR-Chk1 activation, experimental evidence indicates that DNA damage activates the S-phase checkpoints through at least two parallel branches, both being regulated by ATM. It causes sequential activation of several gene products in the order of ATM-Chk2-Cdc25A or ATM-Chk2-(NBS1-MRE11-RAD50), leading to S-phase arrest (23, 40). Because ATM and Chk2 are the key proteins in

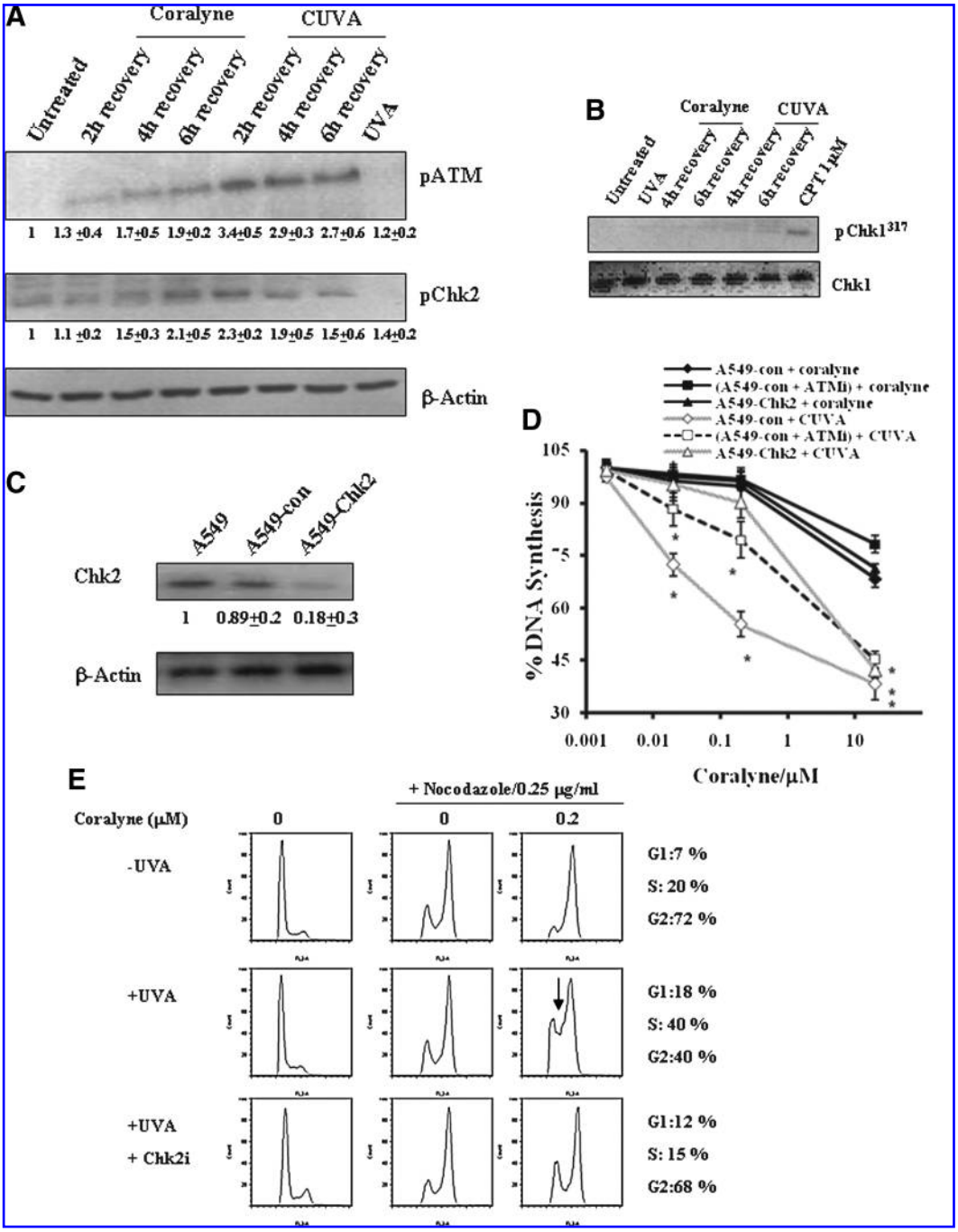

FIG. 11. CUVA-mediated S-phase checkpoint is dependent on ATM and Chk2. (**A**) Western blots of phospho-ATM and phospho-Chk2 in A549 cells after coralyne and CUVA treatment. (**B**) Western blot of phospho-Chk1 in A549 cells after coralyne and CUVA treatment. For (**A**) and (**B**), cell extracts were prepared at 2, 4, or 6 h after the respective treatments. (**C**) Western blots of Chk2. A549, A549-con, and A549-Chk2. (**D**) Effect of ATM/Chk2 downregulation on DNA synthesis. The A549-con, A549-con + ATMi (2 h pretreatment with 10 μM ATMi), and A549-Chk2 cells were treated with coralyne alone or CUVA, and DNA synthesis (S phase) was measured after 2 h with the [^{3}H]thymidine-incorporation assay. *Significantly different compared with the corresponding CUVA-treated A549-ATMi or A549-Chk2 samples by one-way ANOVA ($p < 0.05$). The results are expressed in percentages, considering the value of the corresponding untreated control cells as 1. The experiments were repeated 3 times with similar results. The determinations were made in six replicates, and the *error bars* show the standard errors. (**E**) Cell-cycle analysis for S-phase arrest in response to coralyne and CUVA treatment at 0.2 μM coralyne concentration. In case of Chk2 inhibition, cells were treated with Chk2i (100 nM) throughout the experiment. *Arrow*, Increased accumulation of cells in the S phase in case of CUVA treatment.

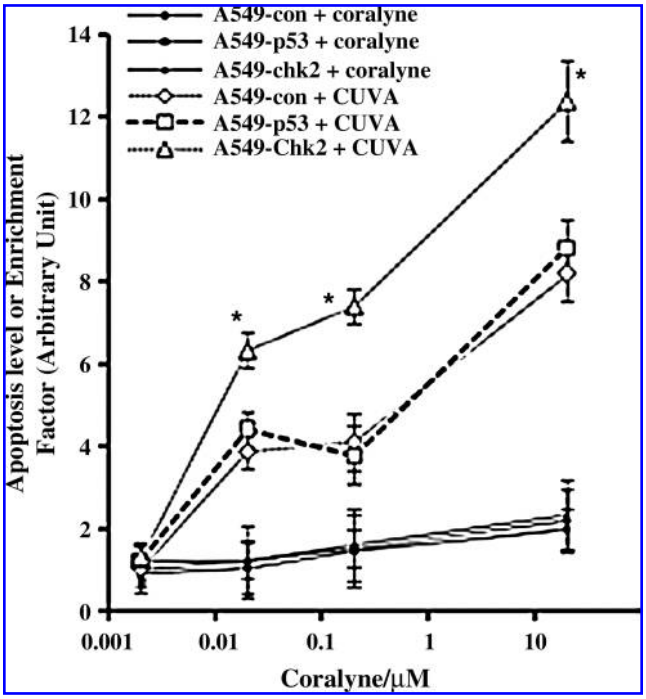

FIG. 12. Effect of p53/Chk2 downregulation on apoptosis. The A549-con, A549-p53, and A549-Chk2 cells were treated with coralyne alone or CUVA, and the enrichment of nucleosomes in cytoplasm was measured after 24 h with ELISA. The results are expressed in percentages, considering the value of the corresponding untreated control cells as 1. The experiment was repeated 3 times with similar results. The determinations were made in six replicates, and the *error bars* show the standard errors.

both the pathways, we envisaged that abrogation of ATM or Chk2 may lead to failure in S-phase arrest, after the CUVA treatment, leading to CUVA-resistant DNA synthesis (CUVADS). Interestingly, ATM autophosphorylation and Chk2 phosphorylation were upregulated severalfold in response to CUVA treatment. Furthermore, Chk2 silencing or ATM protein inhibition resulted in CUVADS and consequent abrogation of S-phase checkpoints in response to the CUVA treatment (at 0.02 and 0.2 μM coralyne). In correlation with these observations, the cell-cycle analyses also showed that CUVA treatment induces S phase, which was defective when Chk2 was inhibited by Chk2-specific inhibitor (Fig. 11E). These results clearly suggested that the CUVA-induced DNA damage elicits S-phase checkpoints by activating the ATM-Chk2 pathway.

Several reports suggested a central role of p53 in determining the sensitivity to apoptosis only when Chk2 is functional (18, 49). Downregulation of Chk2 in cells with functional p53 exhibits resistance to apoptosis in response to DNA damage due to loss of p53 activation. However, because we did not find any change in the sensitivity of A549-p53 cells in response to CUVA (Figs. 5C and 12), this pathway could be excluded. It is generally believed that the p53-defcient cells lacking G_1 arrest enter S and G_2 phases with more-damaged DNA compared with the p53 wild-type cells. Thus, these cells would be dependent more on intact S and G_2 checkpoints to repair DNA damage. However, if the damage is not repairable, Chk2 can activate p53-independent, but p73-dependent apoptosis in response to DNA damage (43). It is of future interest to determine whether the Chk2-mediated p73 pathway is required for CUVA-induced apoptosis.

Conversely, abrogation of S and G_2 checkpoints by downregulating Chk2 or by using G_2 checkpoint abrogators, such as caffeine or UCN-01, is known selectively to sensitize p53-deficient cells to radiation or chemotherapeutic agents (6, 9, 32, 38, 49). Hence, it was of interest to see the role of Chk2, if any, in the p53-independent apoptosis of A549 cells having fully functional p53. Surprisingly, we found that the CUVA treatment results in pronounced apoptosis in the A549-chk2 *vis-à-vis* A549-con and A549-p53 cells (Fig. 12). The results were unexpected but interesting, as A549-chk2 cells have an aborted S-phase checkpoint and showed the CUVADS. This may lead to collision of the replication fork with unrepaired DNA lesions, leading to the formation of DSBs and the consequent death of the cells. Thus, contrary to γ-radiation (18), our results demonstrated, for the first time, that the abrogation of Chk2 could further lead to the CUVA-induced sensitization of p53 wild-type cells.

Besides helping to clarify the action of a novel approach of sensitizing various human cancer cells by CUVA, the results presented here may also be of clinical relevance. Because approximately 50% tumors have defects in the p53 pathway (41), the ability of CUVA to sensitize cells regardless of the p53 status makes the CUVA treatment very potent against a wide range of tumors. Furthermore, CUVA treatment sensitizes cancer cells at extremely low doses of coralyne and UVA, well below the UVA dose required to cause death or mutation if given without the sensitizer (10). Also, its superior efficiency compared with PUVA, and the results of the clonogenic survival assay are very promising. Because coralyne does not absorb in the visible region, UVA light was used for its activation. However, this may not be of much concern because UVA is often used for phototherapy, wherein the laser light is delivered to areas inside the body through fiberoptic cables with an endoscope. This is used to treat even lungs or esophageal cancers. However, issues related to (a) its efficacy in animal models, (b) strategies to deliver coralyne and UVA to internal tumors, as well as (c) the putative mechanism of generation of DSBs and its role in the CUVA-induced apoptosis warrants further investigation.

Author Disclosure Statement

No competing financial interests exist.

References

1. Aas T, Borreson A-L, Geisler S, Smith-Sorenson B, Johnsen H, Varhaug JE, Akslen LA, and Lonning P. Specific P53 mutations are associated with de novo resistance to doxorubicin in breast cancer patients. *Nat Med* 2: 811–814, 1996.
2. Amorino GP, Mikkelsen RB, Valerie K, and Schmidt-Ullrich RK. Dominant-negative cAMP-responsive element-binding protein inhibits proliferating cell nuclear antigen and DNA repair, leading to increased cellular radiosensitivity. *J Biol Chem* 278: 29394–29399, 2003.
3. Antonsson B and Martinou JC. The Bcl-2 protein family. *Exp Cell Res* 256: 50–57, 2000.
4. Bergh J, Norberg T, Slogren S, Lindgren A, and Holmberg L. Complete sequencing of the p53 gene provides prognostic

information in breast cancer patients, particularly in relation to adjuvant systemic therapy and radiotherapy. *Nat Med* 1: 1029–1034, 1995.
5. Bohne C, Faulhaber K, Giese B, Hafner A, Hofmann A, Ihemels H, Pera S, Shneider F, and Sheepwash M. Studies on the mechanism of the photo-induced DNA damage in the presence of acridizinium salts: involvement of singlet oxygen and an unusual source for hydroxyl radicals. *J Am Chem Soc* 127: 76–85, 2005.
6. Bracey TS, Williams AC, and Paraskeva C. Inhibition of radiation-induced G_2 delay potentiates cell death by apoptosis and/or the induction of giant cells in colorectal tumor cells with disrupted p53 function. *Clin Cancer Res* 3: 1371–1381, 1997.
7. Brezova V, Voranova D, and Kostalova D. Oxygen activation by photoexcited protoberberinium alkaloids from *Mahonia aquifolium*. *Phytother Res* 18: 640–644, 2004.
8. Brown KD, Rathi A, Kamath R, Beardsley DI, Zhan Q, Mannino JL, and Baskaran R. The mismatch repair system is required for S-phase checkpoint activation. *Nat Genet* 33: 80–84, 2002.
9. Busby EC, Leistritz DF, Abraham RT, Karnitz LM, and Sarkaria JN. The radiosensitizing agent 7-hydroxystaurosporine (UCN-01) inhibits the DNA damage checkpoint kinase hChk1. *Cancer Res* 60: 2108–2112, 2000.
10. Caffieri S, Di Lisa F, Bolesani F, Facco M, Semenzato G, Dall'Acqua F, and Canton M. The mitochondrial effects of novel apoptogenic molecules generated by psoralen photolysis as a crucial mechanism in PUVA therapy. *Blood* 109: 4988–4994, 2007.
11. Covey JM, Jaxel C, Kohn KW, and Pommier Y. Protein-linked DNA strand breaks induced in mammalian cells by camptothecin, an inhibitor of topoisomerase I. *Cancer Res* 49: 5016–5022, 1989.
12. El-Deiry WS. The role of p53 in chemosensitivity and radiosensitivity. *Oncogene* 22: 7486–7495, 2003.
13. Evan GI and Vousden KH. Proliferation, cell cycle and apoptosis in cancer. *Nature* 411: 342–343, 2001.
14. Falck J, Mailand N, Syljuasen RG, Bartek J, and Lukas J. The ATM-Chk2-Cdc25A checkpoint pathway guards against radioresistant DNA synthesis. *Nature* 410: 842–847, 2001.
15. Gatto B, Sanders MM, Yu C, Wu HY, Makhey D, LaVoie E, and Liu LF. Identification of topoisomerase I as the cytotoxic target of the protoberberine alkaloid coralyne. *Cancer Res* 56: 2795–2800, 1996.
16. Goh H, Yao J, and Smith, D. p53 point mutation and survival in colorectal cancer patients. *Cancer Res* 55: 5217–5221, 1995.
17. Hengartner MO. The biochemistry of apoptosis. *Nature* 407: 770–776, 2000.
18. Hirao A, Kong YY, Matsuoka S, Wakeham A, Ruland J, Yoshida H, Liu D, Elledge SJ, and Mak TW. DNA damage-induced activation of p53 by the checkpoint kinase Chk2. *Science* 287: 1824–1827, 2000.
19. Hirose Y, Berger MS, and Pieper RO. p53 effects both the duration of G_2/M arrest and the fate of temozolomide-treated human glioblastoma cells. *Cancer Res* 61: 1957–1963, 2001.
20. Hsu HF, Houng JY, Kuo CF, Tsao N, and Wu. YC. Glossogin, a novel phenylpropanoid from *Glossogyne tenuifolia*, induced apoptosis in A549 lung cancer cells. *Food Chem Toxicol* 46: 3785–3791, 2008.
21. Ihmels H, Faulhaber K, Sturm C, Bringman G, Gabellini N, Vedaldi D, and Viola G. Acridizinium salts as a novel class of DNA-binding and site-selective DNA-photodamaging chromophores. *Photochem Photobiol* 74: 505–511, 2001.
22. Ihmels H and Salbach A. Efficient photoinduced DNA damage by coralyne. *Photochem Photobiol* 82: 1572–1576, 2006.
23. Kastan MB and Bartek J. Cell-cycle checkpoints and cancer. *Nature* 432: 316–323, 2004.
24. Kastan MB and Lim D. The many substrates and functions of ATM. *Nat Rev* 1: 179–186, 2000.
25. Khanna KK and Jackson SP. DNA double-strand breaks: signaling, repair and the cancer connection. *Nat Genet* 27: 247–254, 2001.
26. Liu L. DNA topoisomerase poisons as antitumor drugs. *Annu Rev Biochem* 58: 351–375, 1989.
27. Lowe SW. Cancer therapy and p53 *Curr Opin Oncol* 7: 547–553, 1995.
28. Miknyoczki SJ, Jones-Bolin S, Pritchard S, Hunter K, Zhao H, Wan W, Ator M, Bihovsky R, Hudkins R, Chatterjee S, and Klein-Szanto A, Dionne C, and Ruggeri B. Chemopotentiation of temozolomide, irinotecan, and cisplatin activity by CEP-6800, a poly(ADP-ribose) polymerase inhibitor. *Mol Cancer Ther* 2: 371–382, 2003.
29. Mosmann T. Rapid colorimetric assay for cellular growth and survival: application to proliferation and cytotoxicity assays. *J Immunol Methods* 65: 55–63, 1983.
30. Painter RB and Young BR. Radiosensitivity in ataxia-telangiectasia: a new explanation. *Proc Natl Acad Sci U S A* 77: 7315–7317, 1980.
31. Pilch DS, Yu C, Markhey D, La Voie EJ, Srinivasan AR, Olson WK, Sauers RR, Breslauer KJ, Geacintov NE, and Liu LF. Minor groove-directed and intercalative ligand-DNA interactions in the poisoning of human DNA topoisomerase I by protoberberine analogs. *Biochemistry* 36: 12542–12553, 1997.
32. Powell SN, DeFrank JS, Connell P, Eogan M, Preįer F, Dombkowski D, Tang W, and Friend S. Differential sensitivity of p53(-) and p53(+) cells to caffeine-induced radiosensitization and override of G_2 delay. *Cancer Res* 55: 1643–1648, 1995.
33. Reelfs O, Xu YZ, Massey A, Karran P, and Storey A. Thiothymidine plus low-dose UVA kills hyperproliferative human skin cells independently of their human papilloma virus status. *Mol Cancer Ther* 6: 2487–2495, 2007.
34. Rojas E, Lopez MC, and Valverde M. Single cell gel electrophoresis assay: methodology and applications. *J Chromatogr B* 722: 225–254, 1999.
35. Schneider E, Hsiang YH, and Liu LF. DNA topoisomerases as anticancer drug targets. *Adv Pharmacol* 21: 149–183, 1990.
36. Seiler JA, Conti C, Syed A, Aladjem MI, and Pommier Y. The intra-S-phase checkpoint affects both DNA replication initiation and elongation: single-cell and -DNA fiber analyses. *Mol Cel Biol* 27: 5806–5818, 2007.
37. Shankaranarayanan P and Nigam S. IL-4 induces apoptosis in A549 lung adenocarcinoma cells: evidence for the pivotal role of 15-hydroxyeicosatetraenoic acid binding to activated peroxisome proliferator-activated receptor γ transcription factor. *J Immunol* 170: 887–894, 2003.
38. Shao RG, Cao CX, Shimizu T, O'Connor PM, Kohn KW, and Pommier Y. Abrogation of an S-phase checkpoint and potentiation of camptothecin cytotoxicity by 7-hydroxystaurosporine (UCN-01) in human cancer cell lines, possibly influenced by p53 function. *Cancer Res* 57: 4029–4035, 1997.

39. Siddik Z. Cisplatin: mode of cytotoxic action and molecular basis of resistance. *Oncogene* 22: 7265–7279, 2003.
40. Sørensen CS, Syljuasen RG, Falck J, Schroeder T, Ronnstrand L, Khanna KK, Zhou B, Bartek J, and Lukas J. Chk1 regulates the S phase checkpoint by coupling the physiological turnover and ionizing radiation-induced accelerated proteolysis of Cdc25A. *Cancer Cell* 3: 247–258, 2003.
41. Soussi T, Dehouche K, and Beroud, C. p53 website and analysis of p53 gene mutations in human cancer: forging a link between epidemiology and carcinogenesis. *Hum Mutat* 15: 105–113, 2000.
42. Stewart GS, Maser RS, Stankovic T, Bressan DA, Kaplan MI, Jaspers NG, Raams A, Byrd PJ, Petrini JH, and Taylor AM. The DNA double-strand break repair gene hMRE11 is mutated in individuals with an ataxia-telangiectasia-like disorder. *Cell* 99: 577–587, 1999.
43. Urist M, Tanaka T, Poyurovsky MV, and Prives C. Chk1 and Chk2 p73 induction after DNA damage is regulated by checkpoint kinases. *Genes Dev* 18: 3041–3054, 2004.
44. Virag L and Szabo C. The therapeutic potential of poly (ADP-ribose) polymerase inhibitors. *Pharmacol Rev* 54: 375–429, 2002.
45. Viola G, Bressanini M, Gabellini N, Vedaldi D, Dall'Acqua F, and Ihmels H. Naphthoquinolizinium derivatives as a novel platform for DNA-binding and DNA-photodamaging chromophores. *Photochem Photobiol Sci* 1: 882–889, 2002.
46. Viola G, Dall'Acqua F, Gabellini N, Moro S, Vedaldi D, and Ihmels H. Indolo[2,3-b]-quinolizinium bromide: an efficient intercalator with DNA-photodamaging properties. *Chem Biochem* 3: 550–558, 2002.
47. Vousden KH and Lu X. Live or let die: the cell's response to p53. *Nat Rev Cancer* 2: 594–604, 2002.
48. Weiss RH. p21Waf1/Cip1 as a therapeutic target in breast and other cancers. *Cancer Cell* 4: 425–429, 2003.
49. Yu Q, Rose JHL, Zhang H, and Pommier Y. Antisense inhibition of Chk2/hCds1 expression attenuates DNA damage-induced S and G_2 checkpoints and enhances apoptotic activity in HEK-293 cells. *FEBS Lett* 505: 7–12, 2001.
50. Zee-Cheng KY and Cheng CC. Solubilization and stabilization of the cytotoxic agent coralyne. *J Med Chem* 19: 882–886, 1976.
51. Zee-Cheng KY, Paull KD, and Cheng CC. Experimental antileukemic agents: coralyne, analogs, and related compounds. *J Med Chem* 17: 347–351, 1974.
52. Zijlstra JG, de-Jong S, de Vries EG, and Mulder NH. Topoisomerases, new targets in cancer chemotherapy. *Med-Oncol Tumor Pharmacother* 7: 11–18, 1990.

Address correspondence to:
Dr. Subrata Chattopadhyay
Bio-Organic Division
Prof. Homi Bhabha National Institute
Bhabha Atomic Research Centre
Mumbai 400085
India

E-mail: schatt@barc.gov.in

Date of first submission to ARS Central, February 14, 2009; date of final revised submission, October 19, 2009; date of acceptance, October 27, 2009.

Abbreviations Used

ATMi = ATM-specific inhibitor
Chk2i = Chk2-specific inhibitor
CPT = camptothecin
[^{14}C]TdR = [^{14}C]Thymidine
CUVA = coralyne plus UVA
CUVADS = CUVA-resistant DNA synthesis
DSB = DNA double-strand break
[^{3}H]TdR = ^{3}H-thymidine
PARP-1 = poly(ADP-ribose) polymerase-1
PUVA = psoralen plus UVA
SSB = single-strand break

This article has been cited by:

1. Sneha Ghadigaonkar, Mrunesh R. Koli, Sunita S. Gamre, Manoj K. Choudhary, Subrata Chattopadhyay, Anubha Sharma. 2012. A chemoenzymatic asymmetric synthesis of (+)-strictifolione. *Tetrahedron: Asymmetry* . [CrossRef]
2. Sucheta Chatterjee, Seema V. Kanojia, Subrata Chattopadhyay, Anubha Sharma. 2011. First asymmetric synthesis of the oxylipin, (6S,9R,10S)-6,9,10-trihydroxyoctadeca-7E-enoic acid. *Tetrahedron: Asymmetry* **22**:3, 367-372. [CrossRef]